Pore-opening mechanism of the nicotinic acetylcholine receptor evinced by proton transfer

Gisela D Cymes & Claudio Grosman

SUPPLEMENTARY INFORMATION

SUPPLEMENTARY FIGURES

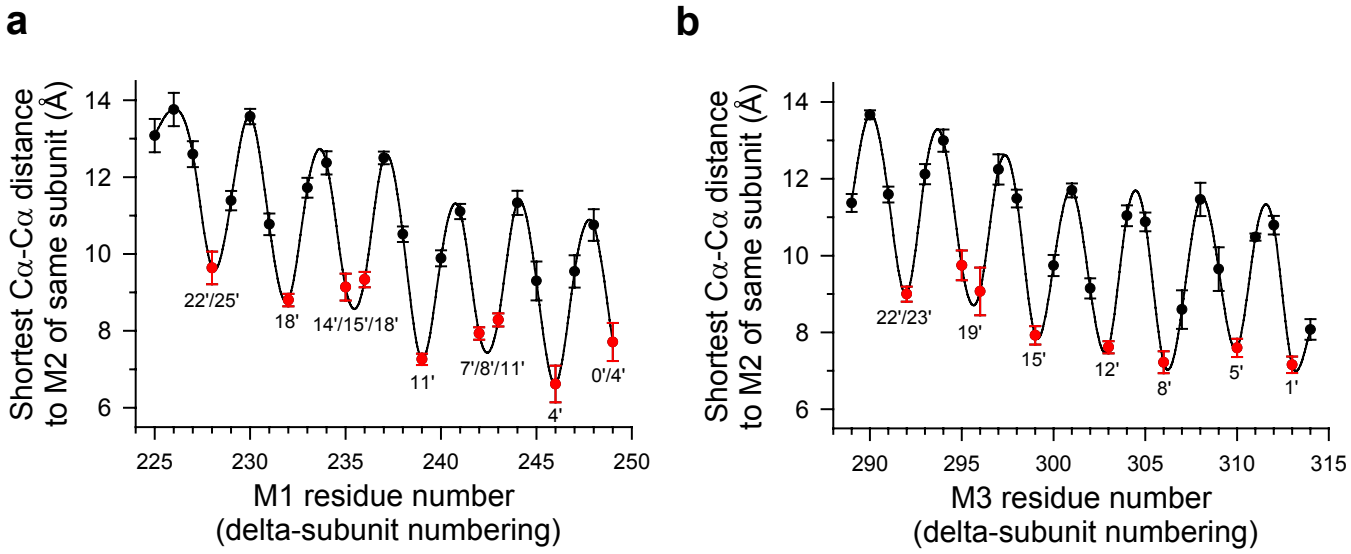

Supplementary Figure 1 Characterization of intrasubunit M1–M2 and M3–M2 interfaces in the closed state. (**a**) All possible intrasubunit Cα–Cα distances between M1 and M2 were measured, and the shortest ones are plotted as a function of M1 residue number. The minima (indicated in red) identify the interfacial positions in M1. The interfacial positions in M2 vary among subunits and are indicated next to these minima using the prime-numbering system. The mean Cα–Cα distance at the intrasubunit M1–M2 interface is (8.3 ± 0.3) Å. (**b**) The mean Cα–Cα distance at the intrasubunit M3–M2 interface is (8.2 ± 0.3) Å. Means and standard errors were calculated from the values corresponding to the five individual subunits, and the unbroken lines are cubic-spline interpolations. All distances were measured on the PDB file 2BG9 (ref. 1) using VMD (ref. 46). A similar analysis of mean interfacial Cα–Cα distances between the M1 and M3 segments of the same and adjacent subunits gives values of (8.7 ± 0.5) Å and (8.4 ± 0.4) Å, respectively.

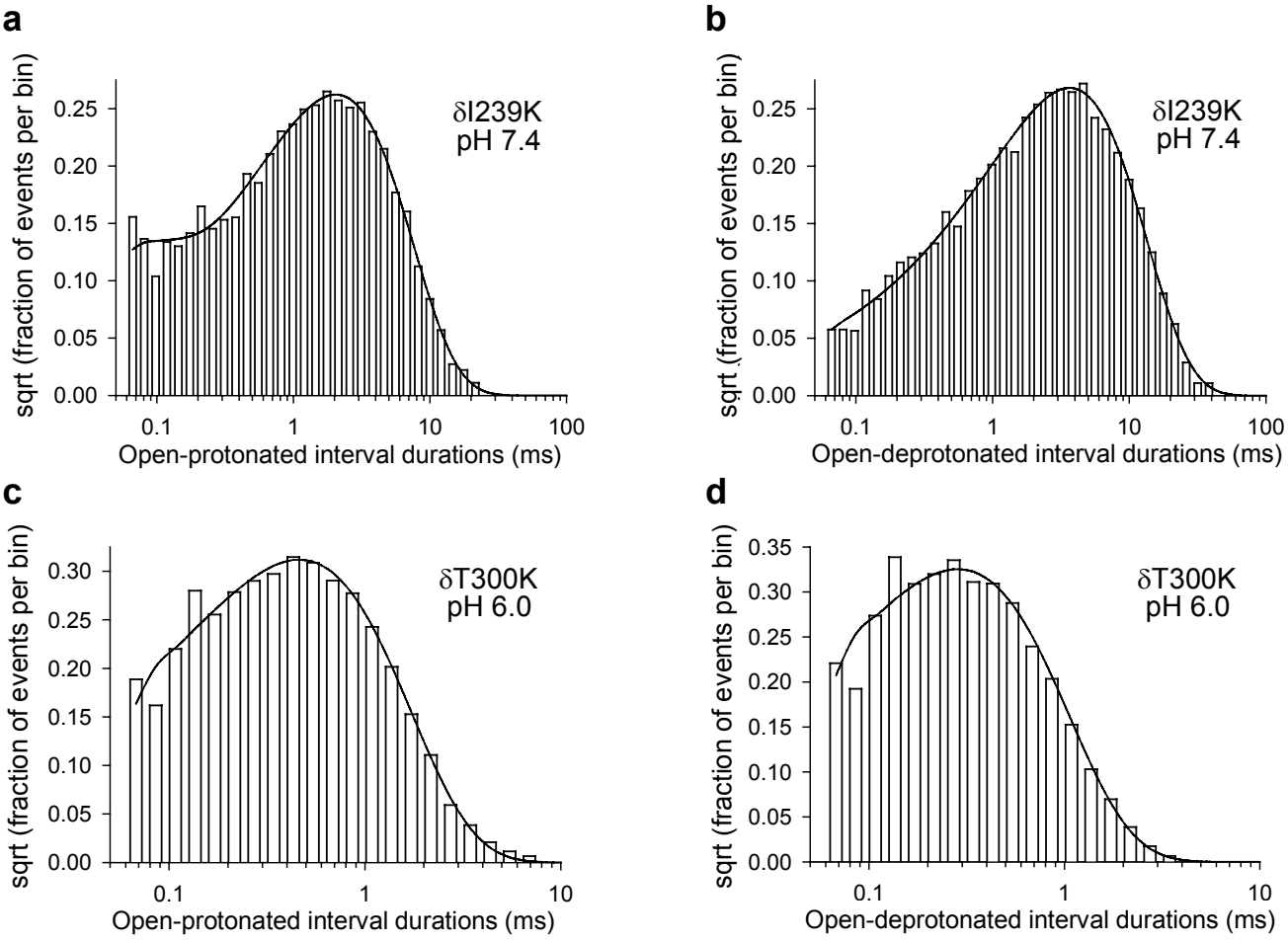

Supplementary Figure 2 Kinetic characterization of proton-transfer events. Dwell-time histograms of the protonated and deprotonated open-channel current levels of two lysine mutants. Superimposed exponential densities (unbroken lines) were computed from the estimates of transition rates with allowance for missed events. In turn, transition rates were estimated from maximum-likelihood fitting of dwell-time series (see Methods) with kinetic models based on that in Figure 6a. Shut-time histograms are not shown. (**a**), (**b**) Histograms corresponding to one representative recording from the δI239K M1 mutant at pH 7.4 and –100 mV (17,207 intervals). The unbroken line in **a** is a double-exponential density whereas that in **b** is a monoexponential density. Time resolution ≅ 50 μs. A representative trace is shown in Figure 3a. The idealized version of this recording contained an excess of short-lived excursions to the open-protonated level preceded and followed by sojourns in the open-deprotonated level (the "main level"). These brief events account for the fast component (time constant

≅ 47 μS; area ≅ 0.056) of the double-exponential distribution in **a**. We favor the notion that, at least to some extent, these brief events correspond to short, unresolved full closures of the channel that are mis-idealized as dwellings in the open-protonated level (the "sublevel"). To account for these events during the fitting of transition rates, and thus, to obtain an accurate estimate of proton-transfer rates, an additional 'open-protonated state' (connected only to the open-deprotonated state) was added to a kinetic scheme like that in Figure 6a. In the particular recording illustrated here, the entry rate into this brief-lived state was ~52 s^{-1}, whereas the exit rate from it was ~21,165 s^{-1}. Thus, the probability of the idealized signal dwelling in this state rather than in the open-deprotonated level from which it originates was extremely low (~0.0025); this was also the case for all other recordings in which short events like these were detected. (**c**), (**d**) Histograms corresponding to one representative recording from the δT300K M3 mutant at pH 6.0 and –150 mV (46,210 intervals). Unbroken lines are monoexponential densities. Time resolution ≅ 50 μs. A representative trace is shown in Figure 3d.

SUPPLEMENTARY TABLE 1 Extent of channel block and pK_a-shifts as probes of pore symmetry

Probed position	Mutation	pH	Deprotonation rate (s^{-1})	Protonation rate (s^{-1})	p$K_{a,\ pore}$	ΔpK_a	Extent of block
α10′ (M2)[a]	S → K	9.0	346 ± 20	9,937 ± 210	10.46 ± 0.03	0.06	0.71
β10′ (M2)	T → K	7.4	134 ± 4	13,069 ± 154	9.39 ± 0.10	–1.01	0.61
δ10′ (M2)	A → K	7.4	1,792 ± 77	2,383 ± 63	7.53 ± 0.01	–2.87	0.51
ε10′ (M2)	A → K	7.4	441 ± 14	7,405 ± 92	8.63 ± 0.01	–1.77	0.68
α12′ (M2)[a]	T → K	7.4	1,636 ± 55	4,057 ± 88	7.80 ± 0.009	–2.60	0.65
β12′ (M2)	T → K	7.4	308 ± 10	13,305 ± 1,212	9.03 ± 0.05	–1.37	0.67
δ12′ (M2)	S → K	7.4	443 ± 11	13,028 ± 345	8.87 ± 0.008	–1.53	0.62
ε12′ (M2)	T → K	7.4	321 ± 30	15,367 ± 1,200	9.08 ± 0.04	–1.32	0.66

All measurements were performed at –100 mV.

[a]The listed proton-transfer rates, pK_as and extent-of-block values correspond to the monoprotonated ⇌ deprotonated step. Protonation rates were calculated as the observed best-fit values divided by 2, as indicated in Figure 6b, to account for the two proton-binding sites in these α1-subunit double-mutant constructs.